Behaviour of $[Ru_2(CO)_4(\mu\text{-}MeCO_2\text{-}O,O')_2(PBu^n{}_3)_2]$ in the Presence of Hydrogen: Synthesis and *X*-Ray Structure of Polynuclear Ruthenium Carbonyl Hydrides containing an Encapsulated Phosphide Ligand *

Piero Frediani, Mario Bianchi, Antonella Salvini, and Franco Piacenti
Dipartimento di Chimica Organica, Università di Firenze, Via Gino Capponi 9, I-50121 Firenze, Italy
Sandra Ianelli and Mario Nardelli
Istituto di Chimica Generale ed Inorganica, Università di Parma e Centro di Studio per la Strutturistica Diffrattometrica del CNR, Viale delle Scienze, I-43100 Parma, Italy

The compound $[Ru_2(CO)_4(\mu\text{-}MeCO_2\text{-}O,O')_2(PBu^n{}_3)_2]$ under hydrogen (170 atm), between 140 and 200 °C, undergoes rearrangements. Several phosphine-and phosphide-substituted ruthenium carbonyl hydrides are formed. Among them, $[Ru_3(\mu\text{-}H)_2(CO)_7(\mu_3\text{-}PBu^n)(PBu^n{}_3)_2]$, $[Ru_6(\mu\text{-}H)_6(\mu\text{-}CO)(CO)_{12}(\mu\text{-}PBu^n{}_2)(PBu^n{}_3)_2(\mu_6\text{-}P)]$, and $[Ru_7(\mu\text{-}H)_8(CO)_{12}(\mu_3\text{-}PBu^n)(\mu\text{-}PBu^n{}_2)(PBu^n{}_3)_3(\mu_6\text{-}P)]$ were isolated and identified. The *X*-ray crystal structure analyses performed on the three new products have shown boat metal clusters for the last two, containing an encapsulated phosphide ligand.

We report the results of an investigation on the behaviour of $[Ru_2(CO)_4(\mu\text{-}MeCO_2\text{-}O,O')_2(PBu^n{}_3)_2]$ (**1**) in hydrocarbon solution, under nitrogen or hydrogen pressure in the temperature range 20—200 °C. This is part of a wider study on a group of ruthenium carboxylates, (**1**), $[Ru(CO)_2(MeCO_2)_2(PBu^n{}_3)_2]$ (**2**), and $[Ru_4(CO)_8(MeCO_2)_4(PBu^n{}_3)_2]$ (**3**), which have been detected in the crude product from the hydrogenation of acetic acid in the presence of $[Ru_4(\mu\text{-}H)_4(CO)_8(PBu^n{}_3)_4]$ (**4**).[1,2] In previous papers on the behaviour of compound (**2**)[3] and of a mixture of (**2**) and (**3**)[4,5] at various temperatures and pressures of hydrogen and carbon monoxide it has been shown that these systems are very sensitive to the working conditions and easily undergo changes in molecular complexity and in the oxidation number of the metal atoms, giving rise to metal cluster complexes.

We have adopted the same i.r. spectroscopic technique previously described to follow the evolution of the system, and the *X*-ray analysis together with the usual analytical procedures to identify and characterize the new products.

Results

Behaviour of $[Ru_2(CO)_4(\mu\text{-}MeCO_2\text{-}O,O')_2(PBu^n{}_3)_2]$ (**1**) *under Nitrogen.*—The i.r. spectrum of a n-heptane solution of compound (**1**) (2.39 mmol dm^{-3}) does not change up to 130 °C. At 140 °C new bands appear at 2 035, 2 030, 1 981, 1 960, 1 938, 1 919, 1 569, and 1 547 cm^{-1} indicative of the presence of (**3**) (20% conversion); free tri-n-butylphosphine is also present in solution [equation (1)].

$$\underset{(1)}{2[Ru_2(CO)_4(\mu\text{-}MeCO_2\text{-}O,O')_2(PBu^n{}_3)_2]} \rightleftharpoons \underset{(3)}{[Ru_4(CO)_8(MeCO_2)_4(PBu^n{}_3)_2]} + 2PBu^n{}_3 \quad (1)$$

Heating of this solution at 160 °C causes a further increase in the concentration of compound (**3**) and a decrease in that one of (**1**) while a light black decomposition product appears.

Table 1. Main products of the reaction between $[Ru_2(CO)_4(\mu\text{-}MeCO_2\text{-}O,O')_2(PBu^n{}_3)_2]$ and H_2[a]

Run	Concentration/ mmol dm^{-3}	T/°C	Prevailing products
1	38	140	(**1**),[b] (**5**),[c] (**7**), (**6**)[d]
2	16	160	(**1**), (**5**),[b] (**7**),[c] (**8**), (**9**)
3	69	180	(**1**), (**7**),[b] (**8**),[c], (**9**), (**10**), (**11**)
4	100	205	(**9**),[c] (**10**)[b]

[a] n-Heptane as solvent, $p(H_2)$ 170 atm, reaction time 72 h. [b] Highest concentration. [c] Second highest concentration. [d] In the crude product, at room condition, compound (**6**) is transformed into (**2**).[3]

Behaviour of $[Ru_2(CO)_4(\mu\text{-}MeCO_2\text{-}O,O')_2(PBu^n{}_3)_2]$ (**1**) *under Hydrogen.*—The behaviour of compound (**1**) in n-heptane solution (2.43 mmol dm^{-3}) under pressure of hydrogen (50 atm at 20 °C) has been investigated at temperatures between 20 and 200 °C. The i.r. spectra are very complex and suggest the presence of new products in solution in concentrations depending on the operating conditions. In order to interpret these spectra in terms of the concentration of the ruthenium carbonyl species present and to identify possible new species formed, we have performed a series of tests, under the same hydrogen pressure, at progressively higher temperatures. In each of these tests, after equilibration of the system, we recorded the i.r. spectra at high pressure and temperature, at high pressure and room temperature, and then after release of the pressure. We then recovered the solute and isolated, when possible, the new species.

The products isolated were analysed by conventional methods and identified by i.r. and n.m.r. spectroscopic investigations and *X*-ray crystal structure determinations as described later. In Table 1 the results are reported of some equilibration experiments with compound (**1**) under 170 atm of H_2 at different temperatures. Below 120 °C (**1**) remains practically unaltered. At 140 °C a slow conversion takes place and $[Ru_4(\mu\text{-}H)_4(CO)_9(PBu^n{}_3)_3]$ (**5**) and $[RuH_2(CO)_2(PBu^n{}_3)_2]$ (**6**) are formed, identified through their i.r. spectra,[3,6] together with a very small amount of another new species later identified as $[Ru_3(\mu\text{-}H)_2(CO)_7(\mu_3\text{-}PBu^n)(PBu^n{}_3)_2]$ (**7**). At

---

* *Supplementary data available:* see Instructions for Authors, *J. Chem. Soc., Dalton Trans.*, 1990, Issue 1, pp. xix—xxii.

Non-S.I. unit employed: atm = 101 325 Pa.

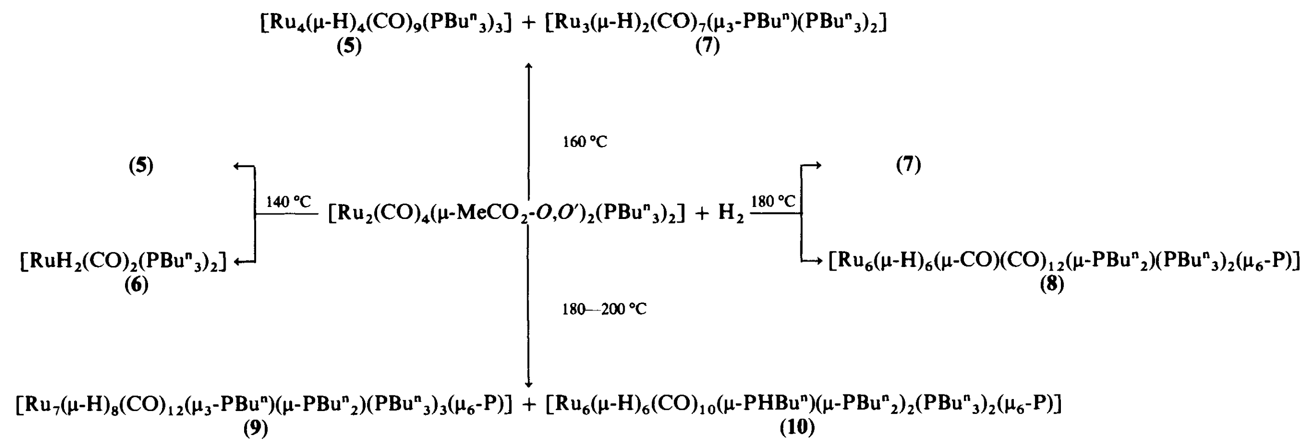

Scheme 1. Prevailing products obtained by reaction of $[Ru_2(CO)_4(\mu\text{-}MeCO_2\text{-}O,O')_2(PBu^n{}_3)_2]$ with H_2

160 °C compound (**5**) is still predominant while the amount of (**7**) increases and the new species $[Ru_6(\mu\text{-}H)_6(\mu\text{-}CO)(CO)_{12}(\mu\text{-}PBu^n{}_2)(PBu^n{}_3)_2(\mu_6\text{-}P)]$ (**8**) and $[Ru_7(\mu\text{-}H)_8(CO)_{12}(\mu_3\text{-}PBu^n)(\mu\text{-}PBu^n{}_2)(PBu^n{}_3)_3(\mu_6\text{-}P)]$ (**9**) become detectable through their i.r. spectra; (**1**) is always present. At 180 °C (**1**) almost completely disappears, (**7**)—(**9**) are still present, and $[Ru_6(\mu\text{-}H)_6(CO)_{10}(\mu\text{-}PHBu^n)(\mu\text{-}PBu^n{}_2)_2(PBu^n{}_3)_2(\mu_6\text{-}P)]$ (**10**)[3] appears together with another new product (**11**) which we have not yet been able fully to characterize. At 200 °C (**10**) becomes predominant while (**9**) is still present in fair concentration.

We would point out that the products reported above, even when predominant, account for only part of the solute: a consistent share of the original complex is transformed into a number of products present in minor amounts which could not be isolated. The best yield, in each reaction, for each product recovered, never exceeds 20% even when the conversion of (**1**) is almost complete. Acetic acid and ethyl acetate were always detected in the crude product after heating at higher temperatures. Butane was detected when the reaction was performed in decalin, at high temperature.

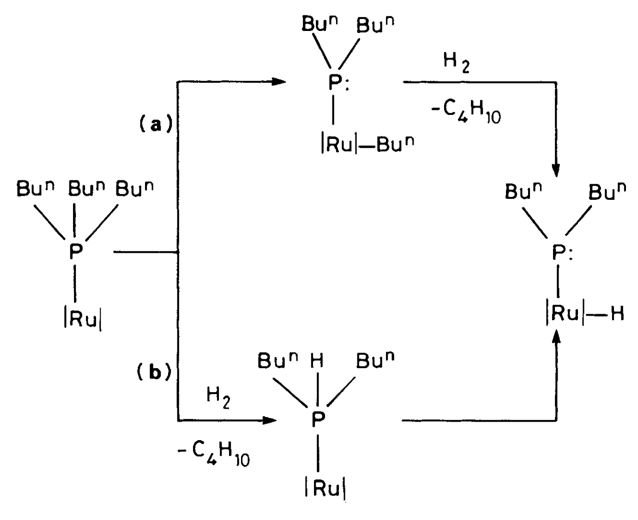

Scheme 2.

X-*Ray Crystal Structure Analyses of Compounds* (**7**)—(**9**).—The final atomic co-ordinates for the non-hydrogen atoms are given in Table 2, relevant bond distances and angles in Table 3.

The hydride hydrogen atoms were located by inspection of the final difference electron-density maps, despite the presence of the heavy ruthenium atoms and of the disorder affecting the terminal methyls of some of the n-butyl chains. After the least-squares refinement without and with these H atoms, the Hamilton[7] significance test was applied (wR and wR' are the weighted R indices for the refinements with and without those hydrogens, respectively): (**7**), $R_{8,4446,0.005} = 1.0025$, $wR'/wR = 1.0402$; (**8**), $R_{48,9761,0.005} = 1.0038$, $wR'/wR = 1.0196$; (**9**), $R_{32,5511,0.005} = 1.0051$, $wR'/wR = 1.0209$. Thus for all three compounds the addition of the hydride hydrogen contributions results in significantly lower R factors. The real presence of these hydrogen atoms was confirmed by ^1H n.m.r. spectroscopy. Calculations with the HYDEX[8] program were carried out to check the co-ordinates obtained from the X-ray analyses and the calculated values are those used in illustrating the results of the structural analyses.

The anisotropic displacement (thermal motion) analysis was carried out in the LST rigid-body approximation of Schomaker and Trueblood[9] considering all the non-H atoms excepting the $CH_2CH_2CH_3$ chain carbons. The rigid-body fits for these parts of the molecules are satisfactory, as shown by the following values of the $R_{wU} = [\Sigma(w\Delta U)^2/\Sigma(wU_o)^2]^{\frac{1}{2}}$ index ($\Delta U = U_{obs.} - U_{calc.}$): (**7**), 0.087; (**8**) (molecule A), 0.089, (molecule B), 0.081; (**9**), 0.113. The bond-distance corrections do not exceed 0.008 Å when Ru and P are involved and 0.011 Å with C and O; they were not considered in the following discussion.

Discussion

(*a*) *Reactivity of the Investigated System.*—Compound (**1**), when heated at 140 °C under nitrogen, gives rise to (**3**), with partial elimination of the phosphine ligand. It reacts with hydrogen under pressure, at appropriate temperatures, giving rise to a number of new hydridic products (Scheme 1). The first and easiest reaction leads, as in the case of the mononuclear derivative (**2**),[3] to loss of the acetato ligand with formation of acetic acid. We have not been able to detect species having both a hydrido and an acetato ligand.

The hydrido species (**5**) and (**6**) in which there is no acetato ligand could be identified only after heating at 140 °C. Tri-n-butylphosphine and carbon monoxide ligands are mobilized too in this transformation. The hydride (**5**) is a tetranuclear cluster. Another rearrangement also takes place and the tri-nuclear hydride (**7**), containing a monoalkylphosphide ligand besides tri-n-butylphosphine, is formed in low concentration. This compound is obtained in higher concentration at 160 °C.

At higher temperatures other trialkylphosphine ligands lose alkyl groups giving rise to $PBu^n{}_2$, $PHBu^n$, PBu^n, and P residues which, because of their higher co-ordination activity, could be

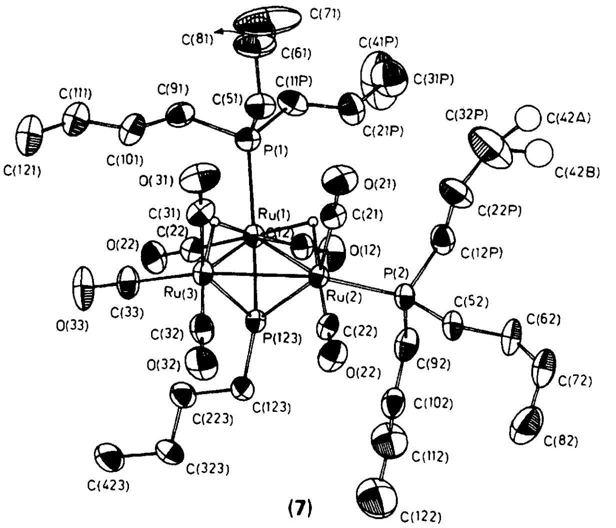

(7)

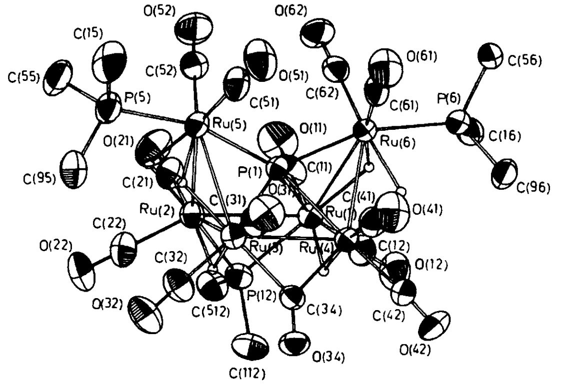

(8) molecule A

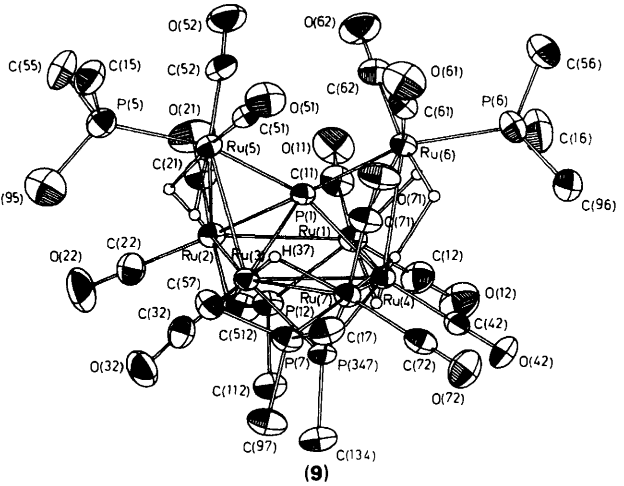

(9)

Figure 1. ORTEP drawings of compounds (**7**), (**8**) (molecule A) and (**9**) showing thermal ellipsoids at 30% probability. For (**8**) and (**9**) the $CH_2CH_2CH_3$ chains of the phosphine ligands are omitted for clarity

responsible, as suggested by Colbran *et al.*,[10] for the formation of the higher nuclearity clusters. All the hydridic species (**8**)—(**10**) formed at temperatures above 160 °C have μ_6-P and μ-$PBu^n{}_2$ ligands.

The bridging position of the hydridic hydrogens is in agreement with their ^1H n.m.r. absorptions that lie between τ 25 and 35. The seven ruthenium atom cluster is particularly interesting because the phosphorus-containing ligands are present in the same molecule with all possible alkylation degrees.

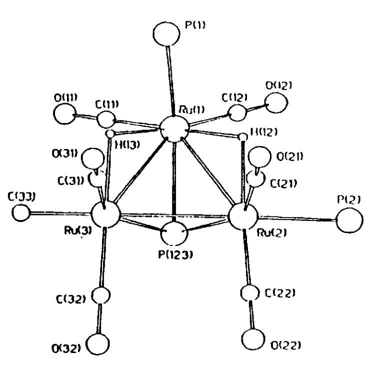

(7)

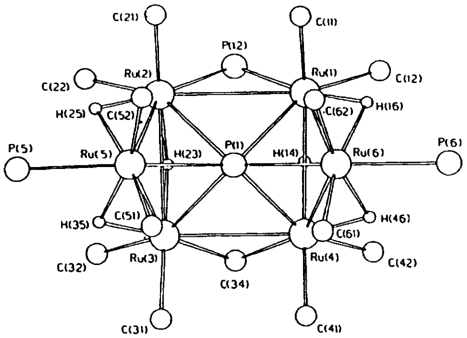

(8) molecule A

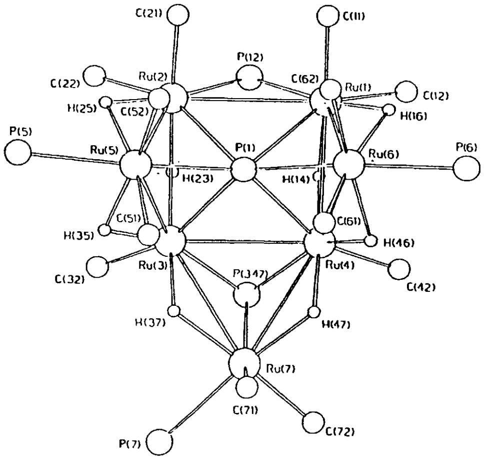

(9)

Figure 2. Projections of the cores of compounds (**7**), (**8**) (molecule A), and (**9**) showing the approximate local symmetries (see text)

The formation of the above clusters apparently takes place through parallel reactions. When taken singularly, they appear relatively stable up to 200 °C in the presence of hydrogen under pressure and also, in the case of (**10**), of acetic acid.

In Scheme 2 we report two possible paths for alkyl elimination from phosphine bound to a ruthenium atom with formation of the above complexes. One way (a) involves the formation of a ruthenium alkyl intermediate by the interaction of a phosphorus–carbon bond of the phosphine with the metal, which is then hydrogenated with elimination of butane and formation of the hydride. The other path (b) involves hydrogenolysis of a phosphorus–carbon bond with butane elimination followed by oxidative addition of the P–H bond to the metal atom. Both reaction paths have previously been suggested.[10–12]

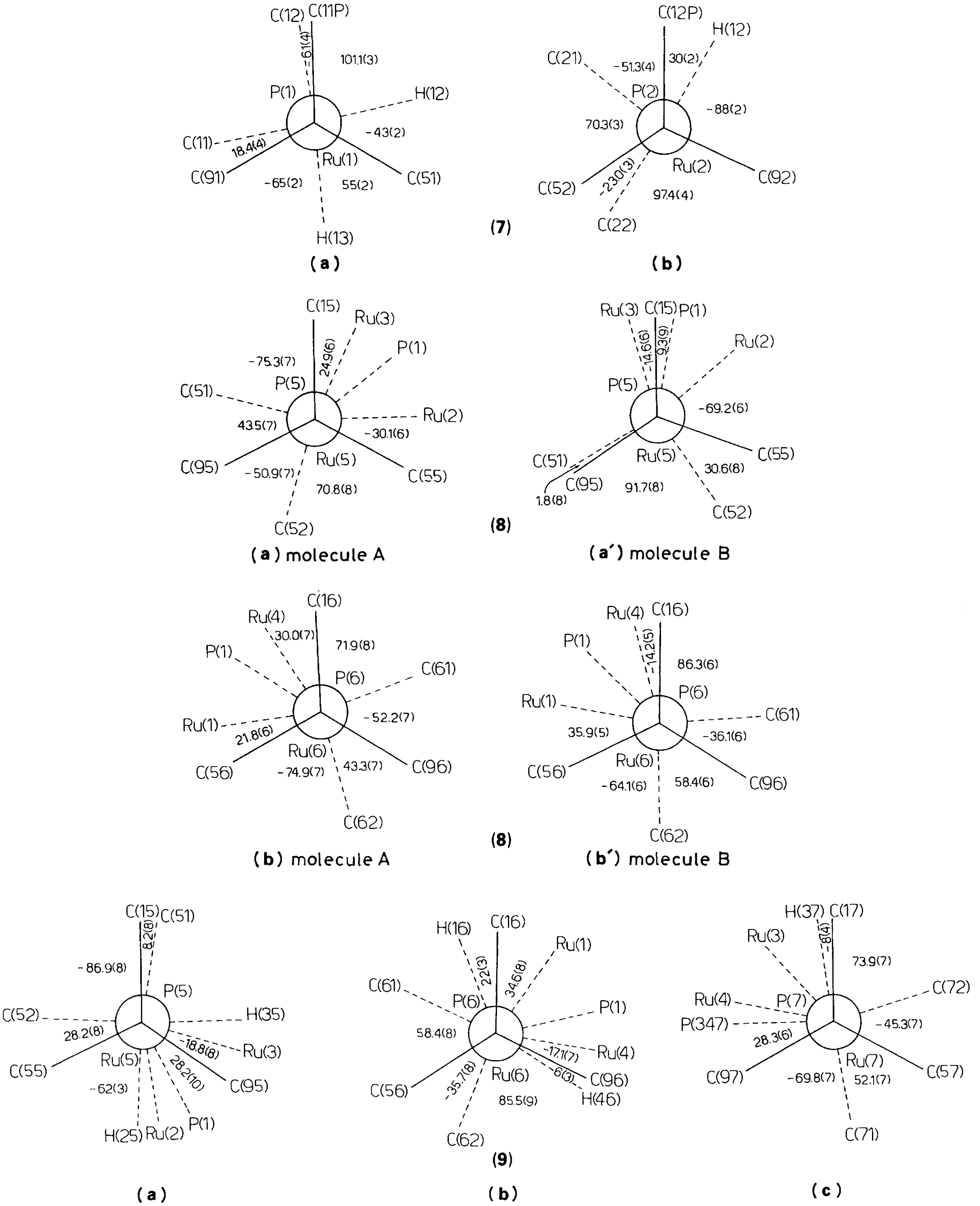

Figure 3. Newman projections showing the orientation of the terminal phosphine ligands with respect to the cores of compounds (7)—(9)

(*b*) X-*Ray Structures*.—[$Ru_3(\mu\text{-}H)_2(CO)_7(\mu_3\text{-}PBu^n)(PBu^n{}_3)_2$] (7). Figure 1 shows the molecular structure of compound (7) which is found to be a 48-electron trinuclear cluster containing one triply bridging mono-n-butylphosphide and two terminal tri-n-butylphosphine ligands. The co-ordination numbers for the three ruthenium atoms are seven for Ru(2) and Ru(3) and eight for Ru(1).

Considering the data of Table 3 it appears that substitution at the ruthenium atoms influences the shape of the metal cluster which deviates from being triangular equilateral, since the Ru(1)–Ru(2) and the Ru(1)–Ru(3) sides, bridged by the hydride hydrogens, are significantly longer than the Ru(2)–Ru(3) unbridged side.

As shown by the projection of the molecular core in Figure 2, the different CO and phosphine substitution at Ru(3) and Ru(2) respectively cancels the approximate mirror symmetry shown by the core with respect to the P(1)–Ru(1)–P(123) plane.

The Newman projections of Figure 3 and the ORTEP drawing of Figure 1 help to evaluate the orientations of the terminal phosphine ligands with respect to the cluster. These orientations are essentially determined by the contacts the butyl chains undergo with the carbonyls.

Table 2. Fractional atomic co-ordinates (× 10^4) with e.s.d.s in parentheses

Atom	*X/a*	*Y/b*	*Z/c*
Compound (**7**)			
Ru(1)	2 514.9(2)	3 653.0(4)	1 276.3(5)
Ru(2)	2 184.8(2)	4 690.3(4)	−1 862.9(5)
Ru(3)	2 012.8(2)	2 393.7(4)	−1 024.4(5)
P(1)	3 510.2(7)	2 774.3(16)	1 360.5(19)
P(2)	2 140.2(8)	6 712.1(14)	−1 657.5(19)
P(123)	1 623.3(7)	4 143.0(13)	194.7(17)
O(11)	2 133(2)	2 333(4)	4 142(5)
O(12)	2 505(3)	5 824(4)	3 134(6)
O(21)	3 207(3)	3 887(5)	−4 171(6)
O(22)	1 358(2)	5 086(4)	−4 438(6)
O(31)	2 970(3)	1 106(6)	−3 269(7)
O(32)	1 047(3)	2 633(6)	−3 214(7)
O(33)	1 643(3)	441(5)	997(7)
C(11)	2 276(3)	2 833(5)	3 073(8)
C(12)	2 506(3)	4 999(6)	2 425(7)
C(21)	2 827(3)	4 227(6)	−3 298(7)
C(22)	1 666(3)	4 946(5)	−3 450(7)
C(31)	2 621(3)	1 574(6)	−2 450(8)
C(32)	1 412(4)	2 534(6)	−2 411(8)
C(33)	1 780(4)	1 173(6)	243(9)
C(11P)	3 983(3)	3 610(7)	2 229(8)
C(21P)	4 024(4)	4 753(8)	1 440(11)
C(31P)	4 424(5)	5 438(11)	2 154(16)
C(41)	4 393(8)	5 557(14)	3 619(20)
C(51)	3 862(3)	2 371(7)	−565(8)
C(61)	4 495(4)	1 753(11)	−646(11)
C(71)	4 747(7)	1 468(19)	−2 223(19)
C(81)	4 642(10)	1 544(26)	−3 491(20)
C(91)	3 655(3)	1 406(7)	2 554(8)
C(101)	3 402(4)	412(7)	2 020(10)
C(111)	3 418(4)	−605(8)	3 214(11)
C(121)	3 154(5)	−1 570(9)	2 692(14)
C(12P)	2 807(3)	7 145(6)	−1 218(9)
C(22P)	3 303(4)	6 816(10)	−2 406(12)
C(32P)	3 843(7)	7 292(20)	−1 932(20)
C(42A)	3 881(12)	8 307(27)	−2 210(33)
C(42B)	4 216(19)	7 655(35)	−2 951(48)
C(52)	1 909(3)	7 591(5)	−3 426(7)
C(62)	1 896(4)	8 917(6)	−3 427(10)
C(72)	1 623(5)	9 547(8)	−4 898(11)
C(82)	999(5)	9 629(10)	−4 918(14)
C(92)	1 658(4)	7 463(6)	−120(8)
C(102)	1 022(4)	7 597(6)	−358(9)
C(112)	644(5)	8 121(10)	1 091(13)
C(122)	15(7)	8 266(12)	815(19)
C(123)	907(3)	4 609(6)	1 185(8)
C(223)	740(3)	3 641(6)	2 280(8)
C(323)	128(3)	3 975(8)	2 992(11)
C(423)	−32(4)	2 976(8)	4 026(12)
Compound (**8**)			
Molecule A			
Ru(1)	3 972.2(5)	8 129.0(4)	−51.6(5)
Ru(2)	2 631.8(5)	8 147.7(4)	948.2(5)
Ru(3)	1 572.3(5)	7 642.1(4)	−487.3(5)
Ru(4)	2 852.9(5)	7 611.2(4)	−1 449.2(5)
Ru(5)	1 883.1(5)	6 816.8(4)	724.2(5)
Ru(6)	3 784.0(5)	6 798.6(4)	−665.2(5)
P(1)	2 793(2)	7 251(1)	−102(2)
P(12)	3 477(2)	8 947(1)	550(2)
P(5)	842(2)	6 663(2)	1 504(2)
P(6)	4 803(2)	6 582(2)	−1 406(2)
O(11)	5 030(6)	8 058(5)	1 393(6)
O(12)	5 248(6)	8 878(4)	−778(6)
O(21)	3 619(6)	8 054(5)	2 443(5)
O(22)	1 656(6)	8 945(5)	1 804(7)
O(31)	492(7)	6 676(5)	−1 641(6)
O(32)	340(6)	8 394(5)	−141(8)
O(41)	1 900(6)	6 632(5)	−2 662(6)
O(42)	3 565(9)	8 272(6)	−2 741(7)
O(51)	1 353(7)	5 576(5)	−286(7)
O(52)	3 011(7)	6 334(6)	1 823(7)
O(61)	2 799(7)	5 549(5)	−1 251(7)
O(62)	4 481(6)	6 462(5)	875(6)
O(34)	1 816(5)	8 563(4)	−1 675(5)
C(11)	4 622(7)	8 085(5)	841(8)
C(12)	4 756(7)	8 596(6)	−498(7)
C(21)	3 269(7)	8 096(6)	1 859(7)
C(22)	2 024(8)	8 638(6)	1 495(8)
C(31)	918(9)	7 043(7)	−1 223(8)
C(32)	762(7)	8 094(6)	−307(9)
C(41)	2 254(8)	7 026(7)	−2 208(7)
C(42)	3 320(10)	8 017(8)	−2 257(9)
C(51)	1 577(8)	6 026(6)	72(8)
C(52)	2 614(8)	6 512(7)	1 401(9)
C(61)	3 170(7)	6 009(6)	−1 006(8)
C(62)	4 196(8)	6 566(5)	298(8)
C(34)	1 997(7)	8 153(6)	−1 369(7)
C(15)	−84(8)	6 761(7)	1 023(11)
C(25)	−367(9)	6 302(8)	288(12)
C(35)	−1 131(13)	6 399(13)	−139(17)
C(45)	−1 394(14)	5 964(12)	−898(14)
C(55)	945(9)	7 191(7)	2 411(11)
Molecule B			
Ru(1)	9 289.5(5)	7 669.5(4)	6 075.4(5)
Ru(2)	7 971.7(5)	6 979.3(4)	4 911.1(5)
Ru(3)	6 891.6(5)	7 284.9(4)	6 089.1(5)
Ru(4)	8 154.9(5)	7 923.8(4)	7 219.9(5)
Ru(5)	7 083.9(5)	7 988.5(4)	4 705.2(5)
Ru(6)	8 931.1(5)	8 932.9(4)	6 392.7(5)
P(1)	8 035(2)	8 059(1)	5 778(2)
P(12)	8 913(2)	6 623(1)	5 637(2)
P(5)	6 031(2)	7 628(2)	3 744(2)
P(6)	9 943(2)	9 562(1)	7 251(2)
O(11)	10 203(6)	7 946(5)	4 712(7)
O(12)	10 696(6)	7 582(5)	7 107(7)
O(21)	8 900(6)	7 135(5)	3 517(5)
O(22)	7 151(7)	5 739(5)	4 072(6)
O(31)	5 723(6)	7 946(5)	6 862(6)
O(32)	5 790(6)	6 062(5)	5 831(7)
O(41)	7 145(6)	8 695(5)	8 077(6)
O(42)	8 951(7)	7 680(5)	8 749(5)
O(51)	6 550(7)	9 158(5)	5 362(7)
O(52)	8 051(7)	8 673(5)	3 586(6)
O(61)	7 841(6)	9 840(5)	6 687(6)
O(62)	9 406(6)	9 367(5)	4 834(6)
O(34)	7 221(4)	6 719(4)	7 584(5)
C(11)	9 847(7)	7 829(6)	5 228(9)
C(12)	10 162(7)	7 607(6)	6 707(8)
C(21)	8 564(7)	7 086(6)	4 064(7)
C(22)	7 463(8)	6 214(7)	4 388(7)
C(31)	6 188(8)	7 711(6)	6 580(7)
C(32)	6 178(7)	6 528(7)	5 942(8)
C(41)	7 510(8)	8 395(6)	7 726(7)
C(42)	8 666(8)	7 791(6)	8 191(7)
C(51)	6 762(7)	8 719(7)	5 107(8)
C(52)	7 701(8)	8 403(6)	3 995(8)
C(61)	8 252(7)	9 502(6)	6 550(7)
C(62)	9 224(7)	9 213(5)	5 423(7)
C(34)	7 369(6)	7 100(5)	7 166(6)
C(15)	5 470(8)	6 892(7)	3 920(8)
C(25)	4 816(11)	6 593(10)	3 257(11)
C(35)	4 417(18)	5 969(15)	3 543(20)
C(45)	4 815(28)	5 471(14)	3 593(29)
C(55)	6 263(10)	7 475(9)	2 730(8)

Table 2 *(continued)*

Atom	*X*/*a*	*Y*/*b*	*Z*/*c*	Atom	*X*/*a*	*Y*/*b*	*Z*/*c*
Compound (**8**)							
Molecule A				Molecule B			
C(65)	1 627(11)	7 157(9)	2 980(10)	C(65)	6 735(11)	6 975(11)	2 583(9)
C(75)	1 748(17)	7 735(20)	3 679(19)	C(75)	6 785(15)	6 696(11)	1 781(12)
C(85)	2 486(28)	7 634(20)	4 184(21)	C(85)	7 274(16)	6 192(12)	1 713(13)
C(95)	617(8)	5 891(7)	1 813(8)	C(95)	5 338(10)	8 171(9)	3 717(12)
C(105)	−90(11)	5 751(8)	2 301(11)	C(105)	4 876(12)	8 209(11)	4 418(13)
C(115)	−332(12)	5 077(9)	2 411(12)	C(115)	4 518(20)	8 785(16)	4 468(22)
C(125)	−1 043(12)	5 018(10)	2 853(13)	C(125)	4 078(23)	8 821(28)	5 212(25)
C(16)	4 638(10)	6 563(8)	−2 479(10)	C(16)	9 916(8)	9 446(6)	8 286(7)
C(26)	3 944(12)	6 103(10)	−2 851(12)	C(26)	9 246(9)	9 674(7)	8 652(8)
C(36)	3 766(19)	6 067(15)	−3 806(17)	C(36)	9 113(10)	9 431(8)	9 469(10)
C(46)	3 747(22)	6 664(16)	−3 989(23)	C(46)	8 511(10)	9 669(10)	9 842(10)
C(56)	5 695(8)	7 142(7)	−1 213(10)	C(56)	10 905(7)	9 404(6)	7 095(8)
C(66)	6 054(10)	7 256(9)	−378(13)	C(66)	11 148(8)	9 509(7)	6 278(10)
C(76)	6 819(14)	7 864(17)	−108(34)	C(76)	11 954(12)	9 365(14)	6 206(14)
C(96)	5 105(10)	5 829(6)	−1 209(10)	C(86)	12 178(19)	9 466(20)	5 499(29)
C(106)	5 787(13)	5 653(10)	−1 636(13)	C(96)	9 996(6)	10 401(5)	7 216(7)
C(116)	6 080(15)	5 087(9)	−1 216(19)	C(106)	10 638(8)	10 833(6)	7 777(9)
C(126)	6 436(17)	5 174(12)	−468(12)	C(116)	10 597(8)	11 515(7)	7 722(11)
C(112)	4 115(7)	9 472(5)	1 330(8)	C(126)	11 254(10)	11 932(7)	8 328(11)
C(212)	3 712(9)	9 889(8)	1 874(11)	C(112)	8 655(7)	6 110(6)	6 402(8)
C(312)	4 260(18)	10 294(12)	2 541(13)	C(212)	8 177(12)	5 467(8)	6 067(10)
C(412)	4 552(24)	10 003(22)	3 056(19)	C(312)	7 868(21)	4 939(15)	6 627(15)
C(512)	3 069(7)	9 471(5)	−76(7)	C(412)	7 636(19)	5 187(11)	7 187(18)
C(612)	3 638(10)	9 792(7)	−586(11)	C(512)	9 570(8)	6 221(6)	5 061(8)
C(712)	3 090(15)	10 186(10)	−1 232(24)	C(612)	10 290(12)	6 134(12)	5 544(12)
C(28A)	3 577(22)	10 407(17)	−1 781(26)	C(712)	10 895(9)	5 900(9)	5 027(13)
C(28B)	3 582(38)	10 481(31)	−961(39)	C(28A)	11 676(19)	5 919(14)	5 392(17)
C(86A)	7 274(28)	7 586(26)	−347(32)	C(28B)	11 384(40)	6 364(34)	4 822(39)
C(86B)	7 415(65)	8 007(52)	218(66)				
Compound (**9**)							
Ru(1)	8 425.7(5)	1 311.0(7)	4 321.7(6)	C(75)	9 193(10)	−1 980(14)	6 941(13)
Ru(2)	8 473.2(5)	812.0(6)	5 687.7(6)	C(85)	9 817(10)	−1 720(16)	6 999(12)
Ru(3)	7 266.4(5)	1 450.1(6)	5 704.5(5)	C(95)	7 657(8)	−286(13)	7 346(9)
Ru(4)	7 213.3(5)	1 870.3(6)	4 364.3(5)	C(105)	7 196(9)	166(12)	7 586(11)
Ru(5)	7 453.6(5)	−252.9(6)	5 675.5(5)	C(115)	7 312(11)	709(14)	8 146(9)
Ru(6)	7 409.3(5)	361.6(6)	3 768.9(5)	C(125)	6 874(10)	1 151(12)	8 363(10)
Ru(7)	6 126.7(5)	1 968.3(6)	4 977.5(5)	C(16)	7 941(9)	616(16)	2 322(9)
P(1)	7 596(2)	623(2)	4 857(2)	C(26)	8 372(10)	20(16)	2 400(9)
P(12)	8 950(2)	1 797(2)	5 223(2)	C(36)	8 958(11)	107(21)	2 105(15)
P(347)	7 043(2)	2 580(2)	5 201(2)	C(46)	9 388(14)	−410(20)	2 257(18)
P(5)	7 504(2)	−874(3)	6 657(2)	C(56)	6 857(9)	−305(10)	2 257(8)
P(6)	7 266(2)	497(3)	2 677(2)	C(66)	6 739(13)	−208(13)	1 532(10)
P(7)	5 591(2)	2 295(2)	5 792(2)	C(76)	6 310(16)	−775(21)	1 132(19)
O(32)	7 278(5)	2 174(7)	6 961(5)	C(86A)	5 814(15)	−677(18)	1 353(17)
O(42)	7 086(5)	3 144(6)	3 407(5)	C(86B)	5 784(20)	−540(25)	726(25)
O(11)	9 363(5)	134(7)	4 077(6)	C(96)	6 859(10)	1 374(10)	2 373(9)
O(12)	8 800(6)	2 395(7)	3 364(6)	C(106)	6 214(11)	1 442(14)	2 507(13)
O(21)	9 072(6)	1 036(8)	6 995(6)	C(116)	5 944(16)	2 444(19)	2 132(14)
O(22)	9 361(5)	−429(6)	5 440(6)	C(126)	5 492(18)	2 290(27)	2 378(20)
O(51)	6 134(5)	−619(7)	5 257(6)	C(17)	5 664(6)	1 634(8)	6 458(6)
O(52)	7 881(5)	−1 711(6)	5 080(6)	C(27)	5 425(7)	793(9)	6 314(8)
O(61)	8 073(6)	−1 169(7)	3 755(6)	C(37)	5 435(10)	297(13)	6 917(10)
O(62)	6 209(5)	−398(7)	3 828(6)	C(47)	5 055(12)	545(18)	7 351(12)
O(71)	5 533(5)	3 220(7)	4 139(6)	C(57)	4 790(5)	2 325(8)	5 533(7)
O(72)	5 259(5)	665(6)	4 518(6)	C(67)	4 368(7)	2 492(10)	6 019(8)
C(32)	7 257(6)	1 865(9)	6 484(8)	C(77)	3 697(7)	2 452(13)	5 780(11)
C(42)	7 130(6)	2 649(8)	3 778(7)	C(87)	3 297(8)	2 553(13)	6 272(10)
C(11)	9 020(6)	569(9)	4 204(7)	C(97)	5 772(6)	3 217(8)	6 178(7)
C(12)	8 662(7)	1 973(10)	3 735(8)	C(107)	5 622(8)	3 943(9)	5 794(9)
C(21)	8 844(7)	951(10)	6 492(8)	C(117)	5 786(11)	4 705(10)	6 144(12)
C(22)	9 031(6)	49(9)	5 519(7)	C(127)	5 612(12)	5 392(13)	5 746(14)
C(51)	6 628(7)	−490(8)	5 401(7)	C(112)	8 806(6)	2 791(8)	5 451(7)
C(52)	7 754(7)	−1 144(8)	5 284(8)	C(212)	9 010(8)	2 997(9)	6 130(8)
C(61)	7 824(7)	−602(9)	3 772(8)	C(312)	8 963(8)	3 854(10)	6 307(10)
C(62)	6 659(7)	−121(9)	3 810(7)	C(412)	9 344(11)	4 362(11)	6 026(12)
C(71)	5 752(6)	2 752(8)	4 454(7)	C(512)	9 768(5)	1 766(8)	5 321(7)
C(72)	5 585(6)	1 137(8)	4 706(7)	C(612)	10 079(7)	2 391(11)	4 985(11)
C(15)	6 844(8)	−1 450(10)	6 780(8)	C(712)	10 722(7)	2 466(12)	5 119(15)
C(25)	6 688(10)	−2 138(10)	6 382(11)	C(812)	11 021(9)	3 150(12)	4 907(14)
C(35)	6 074(15)	−2 474(20)	6 429(16)	C(134)	7 226(6)	3 582(7)	5 434(7)
C(45)	5 834(18)	−2 655(23)	6 878(16)	C(234)	7 090(11)	4 171(8)	4 903(8)
C(55)	8 089(8)	−1 631(11)	6 789(10)	C(334)	7 283(18)	5 012(10)	5 092(12)
C(65)	8 704(9)	−1 356(13)	6 842(11)	C(434)	7 185(19)	5 574(15)	4 668(14)

Table 3. Relevant bond distances (Å) and angles (°)

Compound (**7**)

Ru(1)–Ru(2)	2.986(2)	Ru(2)–Ru(1)–Ru(3)	57.2(1)	Ru(1)–C(11)	1.901(7)	Ru(1)–C(12)	1.876(7)
Ru(1)–Ru(3)	2.954(2)	Ru(1)–Ru(2)–Ru(3)	60.8(1)	Ru(2)–C(21)	1.903(6)	Ru(2)–C(22)	1.869(7)
Ru(2)–Ru(3)	2.844(2)	Ru(1)–Ru(3)–Ru(2)	62.0(1)	Ru(3)–C(31)	1.949(7)	Ru(3)–C(32)	1.895(8)
			av. 60.0(14)	Ru(3)–C(33)	1.907(8)		av. 1.879(7)
					av. 1.914(11)		
Ru(1)–P(123)	2.324(2)	Ru(1)–P(1)	2.384(2)	P–C	1.836(4) (av.)	C–P–C	103.0(7) (av.)
Ru(2)–P(123)	2.300(2)	Ru(2)–P(2)	2.343(2)	C–O	1.140(5) (av.)	C–C	1.525(6) (av.)
Ru(3)–P(123)	2.310(2)		av. 2.364(20)				
	av. 2.311(7)						
P(1)–Ru(1)–P(123)	156.1(1)	P(2)–Ru(2)–P(123)	106.8(1)				
P(1)–Ru(1)–Ru(2)	113.2(1)	C(33)–Ru(3)–P(123)	106.7(2)				
P(1)–Ru(1)–Ru(3)	108.1(1)						

P(123) ··· [Ru(1), Ru(2), Ru(3)] 1.576(2)

Cone angle: Ru(1)–P(1)$\mathrm{Bu}^n{}_3$ 150, Ru(2)–P(2)$\mathrm{Bu}^n{}_3$ 139

Compound (**8**)

	Molecule A	Molecule B		Molecule A	Molecule B
Ru(1)–Ru(2)	3.037(2)	3.035(2)	Ru(3)–Ru(4)	2.911(2)	2.909(2)
	av. 3.036(2)			av. 2.910(2)	
Ru(1)–Ru(4)	2.984(2)	2.986(2)	Ru(2)–Ru(3)	2.970(2)	2.980(2)
Ru(1)–Ru(6)	2.936(2)	2.936(2)	Ru(2)–Ru(5)	2.964(2)	2.951(2)
Ru(4)–Ru(6)	2.975(2)	2.958(2)	Ru(3)–Ru(5)	2.971(2)	2.970(2)
	av. 2.962(9)			av. 2.968(4)	
Ru(2)–Ru(1)–Ru(4)	88.4(1)	88.7(1)	Ru(1)–Ru(2)–Ru(3)	89.1(1)	88.9(1)
Ru(1)–Ru(4)–Ru(3)	91.3(1)	91.2(1)	Ru(2)–Ru(3)–Ru(4)	91.1(1)	91.2(1)
	av. 89.9(8)			av. 90.1(6)	
Ru(4)–Ru(1)–Ru(6)	60.3(1)	59.9(1)	Ru(3)–Ru(2)–Ru(5)	60.1(1)	60.1(1)
Ru(1)–Ru(4)–Ru(6)	59.0(1)	59.2(1)	Ru(2)–Ru(3)–Ru(5)	59.9(1)	59.5(1)
Ru(1)–Ru(6)–Ru(4)	60.6(1)	60.9(1)	Ru(2)–Ru(5)–Ru(3)	60.1(1)	60.4(1)
	av. 60.0(3)			av. 60.0(1)	
Ru(1)–P(1)	2.589(3)	2.552(3)	Ru(5)–P(1)	2.376(3)	2.374(3)
Ru(2)–P(1)	2.574(3)	2.624(3)	Ru(6)–P(1)	2.370(3)	2.367(3)
Ru(3)–P(1)	2.530(3)	2.551(3)		av. 2.372(2)	
Ru(4)–P(1)	2.518(3)	2.512(3)			
	av. 2.550(13)				
Ru(6)–P(6)	2.366(4)	2.373(3)	Ru(1)–P(12)	2.296(3)	2.300(3)
Ru(5)–P(5)	2.362(4)	2.366(4)	Ru(2)–P(12)	2.308(3)	2.298(4)
	av. 2.368(2)			av. 2.301(3)	
Ru(5)–P(5)–C(15)	115.1(6)	112.9(5)	Ru(6)–P(6)–C(16)	116.2(6)	114.5(5)
Ru(5)–P(5)–C(55)	114.7(6)	116.0(6)	Ru(6)–P(6)–C(56)	116.6(5)	115.5(4)
Ru(5)–P(5)–C(95)	115.6(5)	113.1(6)	Ru(6)–P(6)–C(96)	111.9(5)	113.8(4)
	av. 114.5(5)			av. 114.7(7)	
Ru–C(CO terminal)	1.882(5) (av.)		Ru–C(CO bridge)	2.080(6) (av.)	
P–C	1.833(4) (av.)		C–P–C	104.0(6) (av.)	
C–O	1.140(4) (av.)		C–C	1.543(10) (av.)	

Cone angle: (molecule A, B) Ru(5)–P(5)$\mathrm{Bu}^n{}_3$ 146, 148; Ru(6)–P(6)$\mathrm{Bu}^n{}_3$ 138, 143.

Compound (**9**)

Ru(1)–Ru(2)	3.069(2)				
Ru(1)–Ru(4)	2.923(2)	Ru(2)–Ru(3)	2.950(2)	Ru(3)–Ru(4)	2.979(2)
Ru(1)–Ru(6)	2.947(2)	Ru(2)–Ru(5)	2.945(2)	Ru(3)–Ru(7)	2.981(2)
Ru(4)–Ru(6)	2.955(2)	Ru(3)–Ru(5)	2.959(2)	Ru(4)–Ru(7)	2.949(2)
	av. 2.942(10)		av. 2.951(4)		av. 2.970(10)

Ru(2)–Ru(1)–Ru(4)	88.7(1)	Ru(1)–Ru(2)–Ru(3)	89.5(1)
Ru(1)–Ru(4)–Ru(3)	91.8(1)	Ru(2)–Ru(3)–Ru(4)	89.9(1)
	av. 90.2(16)		av. 89.7(2)

Table 3 (*continued*)

Ru(4)–Ru(1)–Ru(6)	60.4(1)	Ru(3)–Ru(2)–Ru(5)	60.3(1)	Ru(4)–Ru(3)–Ru(7)	59.3(1)
Ru(1)–Ru(4)–Ru(6)	60.2(1)	Ru(2)–Ru(3)–Ru(5)	59.8(1)	Ru(3)–Ru(4)–Ru(7)	60.4(1)
Ru(1)–Ru(6)–Ru(4)	59.4(1)	Ru(2)–Ru(5)–Ru(3)	60.0(1)	Ru(3)–Ru(7)–Ru(4)	60.3(1)
	av. 60.0(3)		av. 60.0(1)		av. 60.0(4)
Ru(1)–P(1)	2.615(4)	Ru(5)–P(1)	2.380(4)		
Ru(2)–P(1)	2.525(4)	Ru(6)–P(1)	2.382(4)		
Ru(3)–P(1)	2.511(4)		av. 2.381(3)		
Ru(4)–P(1)	2.498(4)				
	av. 2.537(26)				
Ru(5)–P(5)	2.368(5)	Ru(1)–P(12)	2.307(4)	Ru(3)–P(347)	2.252(4)
Ru(6)–P(6)	2.356(4)	Ru(2)–P(12)	2.308(4)	Ru(4)–P(347)	2.258(4)
Ru(7)–P(7)	2.334(4)		av. 2.308(4)	Ru(7)–P(347)	2.321(4)
	av. 2.350(10)				av. 2.277(22)
Ru(5)–P(5)–C(15)	115.2(6)	Ru(6)–P(6)–C(16)	115.1(7)	Ru(7)–P(7)–C(17)	116.4(5)
Ru(5)–P(5)–C(55)	113.9(6)	Ru(6)–P(6)–C(56)	114.8(6)	Ru(7)–P(7)–C(57)	111.5(5)
Ru(5)–P(5)–C(95)	118.3(7)	Ru(6)–P(6)–C(96)	116.0(6)	Ru(7)–P(7)–C(97)	116.8(5)
	av. 115.6(13)		av. 115.3(4)		av. 114.9(17)
Ru(1)–P(12)–C(112)	118.6(5)			Ru(3)–P(347)–C(134)	130.5(5)
Ru(1)–P(12)–C(512)	119.2(5)			Ru(4)–P(347)–C(134)	132.4(5)
Ru(2)–P(12)–C(112)	117.4(5)			Ru(7)–P(347)–C(134)	130.5(5)
Ru(2)–P(12)–C(512)	116.8(5)				av. 131.1(6)
	av. 118.0(5)				
Ru–C(CO terminal)	1.881(12) (av.)				
P–C	1.829(4) (av.)			C–P–C	103.0(7) (av.)
C–O	1.142(6) (av.)			C–C	1.530(15) (av.)

Cone angle: Ru(5)–P(5)$\mathrm{Bu^n_3}$ 142, Ru(6)–P(6)$\mathrm{Bu^n_3}$ 145, Ru(7)–P(7)$\mathrm{Bu^n_3}$ 139

$[\mathrm{Ru_6(\mu\text{-}H)_6(\mu\text{-}CO)(CO)_{12}(\mu\text{-}PBu^n_2)(PBu^n_3)_2(\mu_6\text{-}P)}]$ **(8)**. The crystals of compound (**8**) are built up by two crystallographically non-equivalent 92-electron molecules containing hexanuclear ruthenium clusters in which three kinds of phosphorus atoms are present: a bare phosphorus partially encapsulated in the metal cluster, a symmetrically bridging phosphorus of a phosphide ligand, and two terminal phosphine ligands. One bridging and twelve terminal carbonyl ligands and six bridging hydride hydrogens complete the co-ordination about the metal atoms (Figure 1). The two molecules are chemically equivalent, the crystallographic lack of equivalence being due only to the different folding and orientation of the alkyl chains of the phosphide and phosphine ligands (in Figures 1 and 2 only molecule A is represented).

The shape of the metal cluster can be described as a 'square-boat' with triangular equivalent 'bow' and 'stern' forming a dihedral angle of 104.9(6)° (av.) with the planar base of the 'boat'. This boat conformation can be considered as derived by breaking one of the bonds of a trigonal prism cluster structure caused by the insertion of the phosphide atom.

The four ruthenium atoms at the base are nine-co-ordinated, while the co-ordination number of those at the apices of the bow and stern is eight. All the ruthenium atoms are bound to the central phosphide and, in addition, two of them are bound to the phosphide bridge at the base and two to a phosphine at each apex. The metal co-ordination is completed by two terminal carbonyls bonded to each ruthenium, by a bridging carbonyl symmetrically joining the two metal atoms not involved in the phosphido bridging at the base of the boat, and by the bridging hydride atoms at each edge of the bow and stern triangles.

Both independent molecules, not considering the butyl chains, have a C_v—*m* local approximate symmetry with a pseudo-mirror running through the central and the bridging phosphorus atoms and through the carbon atom of the bridging carbonyl. Moreover, if also the bridging phosphide and carbonyl groups are disregarded, the local symmetry is approximately C_{2v}—*mm*2. This cluster could be conceived as derived from that of $[\mathrm{Ru_6(\mu\text{-}H)_6(CO)_{10}(\mu\text{-}PHBu^n)(\mu\text{-}PBu^n_2)_2(PBu^n_3)_2(\mu_6\text{-}P)}]$ (**10**)[3] by eliminating the phosphide bridging the Ru(2)–Ru(4) edge and pushing down Ru(1) and Ru(3) in the same plane with Ru(2) and Ru(4) which become further apart.

As shown in Table 3, the Ru–Ru distances in the cluster are not all equal; there are significant differences which can be justified by the interactions exerted by the ligands on the metal atoms. In particular the Ru–Ru distance between the ruthenium atoms bridged by the di-n-butylphosphide ligand is larger [3.037(2) and 3.035(2) Å] than all the others, while that between the ruthenium atoms bridged by the carbonyl is the shortest [2.911(2) and 2.909(2) Å]. The remaining Ru–Ru distances are those of the bow and stern triangles which are approximately equilateral [Ru–Ru 2.964(5) Å (av.), Ru–Ru–Ru 60.0(2)° (av.)].

As observed for compound (**10**), the phosphide atom P(4) is only partially encapsulated and its further entry into the cluster is blocked up by the interactions with Ru(5) and Ru(6). Its distances from the Ru atoms at the base are therefore longer: the increase in these distances is proportional to the distances along the direction P(1) ··· [midpoint of Ru(1), Ru(2), Ru(3), Ru(4)]. The Ru–P distances involving the bridging phosphide ligand [2.301(3) Å (av.)] are only slightly shorter than the shortest ones involving the central phosphide atom, while those involving the terminal phosphine [2.368(2) Å (av.)] are practically equal to them.

The orientation of the Ru–P(phosphine) bonds is defined by the angles P(phosphine)–Ru–C(carbonyl) 95.5(6) (av.), P(phosphine)–Ru–Ru 110.3(4) (av.), P(phosphine)–Ru–P(phosphide) 163.2(7)° which are practically equal in both independent molecules and in the two parts of each molecule. On the contrary, the conformation about the P(phosphine)–Ru bonds differs for the two molecules and, in the case of molecule B, also in the two approximately symmetrical parts of the two molecules, as shown by the Newman projections of Figure 3. These differences are due to the different environments of the phosphine ligands and the different folding of the n-butyl chains. A quantitative measurement of the steric hindrance of these bulky ligands is given by Tolman's[13] 'effective' cone angles* whose values are quoted in Table 3 for the terminal tri-n-butylphosphines in all the three compounds.

$[Ru_7(\mu\text{-}H)_8(CO)_{12}(\mu_3\text{-}PBu^n)(\mu\text{-}PBu^n{}_2)(PBu^n{}_3)_3(\mu_6\text{-}P)]$ (**9**). The cluster (**9**) (Figure 1) can be described as derived from that of compound (**8**) by substituting the bridging and two terminal carbonyls, at the Ru(3)–Ru(4) side of the base of the 'boat,' with one bridging ruthenium, Ru(7), carrying a terminal phosphine and carbonyl, and by triply bridging the Ru(3),Ru(4),Ru(7) atoms with a mono-n-butylphosphide ligand. The resulting total electron count of the cluster increases to 106.

The basal plane of the 'boat' is not strictly planar, but shows a slight tetrahedral deformation [±0.029(2) Å]. Atom Ru(7) does not exactly lie in that plane, but the Ru(3)–Ru(4)–Ru(7) triangle makes a dihedral angle of 9.4(1)° with it. Not considering the n-butyl chains and the phosphine and a carbonyl bound to Ru(7), the local approximate symmetry of the cluster is C_s—*m*, with the mirror running through C(71),Ru(7),P(347),P(1),P(12), as shown by the projection of Figure 2.

The co-ordination number is not the same for all the ruthenium atoms, being eight for Ru(5), Ru(6), and Ru(7), nine for Ru(1) and Ru(2), and ten for Ru(3) and Ru(4). As for compound (**8**) the hydridic bridges are placed on the sides of the metal cluster not already subtended by other bridging ligands.

The values of the Ru–Ru distances quoted in Table 3 agree with the local approximate *m* symmetry of the cluster and the Ru(1)–Ru(4)–Ru(6), Ru(2)–Ru(3)–Ru(5), and Ru(3)–Ru(4)–Ru(7) triangles are nearly equilateral [Ru–Ru 2.954(18) Å (av.), Ru–Ru–Ru 60.0(5)° (av.)].

As observed for compounds (**8**) and (**9**), P(1) is only partially encapsulated in the boat part of the cluster that affects its distances to the Ru atoms of the boat, which linearly increase with distance from the base of the boat.

The orientation of the Ru–P (phosphine) bonds at Ru(5) and Ru(6) is similar to that found in compound (**8**) as shown by the values of the angles P(phosphine)–Ru–C(carbonyl) 95.0(6) (av.), P(phosphine)–Ru–Ru 111.1(12) (av.), and P(phosphine)–Ru–P(phosphide) 163.4(1)° (av.), and similar comments can be made about the conformations of the P(phosphine)–Ru bonds, as shown by the Newman projections of Figure 3.

(*c*) *N.M.R. Spectral Properties*.—The interpretation of the n.m.r. data for the new complexes is difficult even when the *X*-ray structures have been successfully determined. This is due not only to the complexity of the systems but also to the scarcity and ambiguity of the information found in the literature on systems of this type. Electronic and steric factors have such a relevant influence on the chemical shifts associated with these ligands[14–16] that we cannot rely on such a parameter to identify the various phosphorus-containing ligands.

The number of hydridic hydrogens in the new compounds has been evaluated by ^1H n.m.r. spectroscopy using (**4**) as internal standard.

The hydridic hydrogen pattern in the ^1H n.m.r. spectrum of compound (**7**) may be interpreted in terms of two signals, the first one at τ 29.3 due to a AXWM system where A = H(12),† and X, W, and M are the phosphorus ligands, with coupling constants $J_{AX} = J_{AW} = 9.0$ and $J_{AM} = 18$ Hz, and the second signal at τ 29.1 due to a BXW system where B = H(13), and X and W are the $PBu^n{}_3$ and PBu^n ligands with coupling constants of $J_{BX} = J_{BW} = 13.5$ Hz. The ^{31}P n.m.r. spectrum may be interpreted in terms of an AX spin system where one of the two groups is the phosphine P(1) ligand coupled with the phosphide ligand P(123) giving a signal at 10.7 p.p.m. (d, $J_{AX} = 97$ Hz) and the other is the phosphide ligand itself giving a signal at 287.7 p.p.m. The signal at 10.7 p.p.m. is attributed to P(1) [the angle P(1)Ru(1)P(123) is 156.1°] in accord with the conclusions of Krassowski *et al.*,[17] that *trans* phosphines (PRuP) have couplings larger than 50 Hz. The phosphine P(2) is neither coupled with the other one located on a different ruthenium atom nor with the phosphide ligand, due to a small P(2)Ru(2)P(123) angle (106°), and gives a singlet at 24.7 p.p.m.

The pattern of the hydridic hydrogens in the ^1H n.m.r. spectrum of compound (**8**) may be interpreted, since the molecule has a local plane of symmetry, in terms of a ABCXMW spin system where A = H(16), B = H(46), C = H(14), and X, M, and W are respectively the trialkylphosphine, the dialkylphosphide, and the phosphide ligands. The signal at τ 25.1 may be attributed to hydrogen A coupled with W (d, $J_{AW} = 20.7$ Hz) with X (d, $J_{AX} = 10.3$ Hz), with M (d, $J_{AM} = 10.3$ Hz), and with hydrogen B (d, $J_{AB} = 3.9$ Hz). The signal at τ 25.7 may be attributed to hydrogen B coupled with X (d, $J_{BX} = 11.8$ Hz), with W (d, $J_{BW} = 11.5$ Hz), and with hydrogen A (d, $J_{AB} = 3.9$ Hz). The signal at τ 33.6 may be attributed to hydrogen C coupled with W (d, $J_{CW} = 18.2$ Hz) and with M (d, $J_{CM} = 9.5$ Hz). The lack of H,H coupling of this last signal and its chemical shift at much higher field than the other two suggest it as due to H(14): the other two hydridic hydrogens are placed in a very similar environment and their chemical shifts should be comparable. The ^{31}P n.m.r. spectrum shows a A_2X spin system with signals at 20.0 (d, 2 P, $PBu^n{}_3$, $J_{AX} = 134$ Hz), 204.3 (t, 1 P, P, $J_{AX} = 134$ Hz), and 197.3 p.p.m. (s, 1P, $PBu^n{}_2$). These couplings are in agreement with the above hypothesis. The phosphide P(1) is coupled with the phosphines P(6) and P(5) because the P(1)Ru(6)P(6) and the P(1)Ru(5)P(5) angles are not far from 180 °C [av. 163.2(7)°]. On the other hand the angles between P(1)Ru(1)P(12) and P(1)Ru(2)P(12) are not far from 90° [av. 98.8°] and there is no coupling.

The ^{31}P n.m.r. spectrum of compound (**9**) shows signals at 3.1 (d), 16.4—24.4 (m), 189.8 (s), 191.2 (s), 219.9 (t), 229.9 (t), 348.2 (s), and 353.5 p.p.m. (d) suggesting the presence in solution of at least two isomeric forms.

Experimental

G.l.c. analyses were performed with a Perkin-Elmer Sigma 1 system. G.l.c.–m.s. spectra were obtained using a Hewlett Packard model 5790 detector connected with a model 5970 capillary gas–liquid chromatograph. Proton, ^{13}C, and ^{31}P n.m.r. spectra were recorded on a Varian CFT80 or VXR300 spectrometer; $SiMe_4$ was used as an external standard for ^1H

---

* Calculated as twice the angle formed by the Ru–P direction and the tangent from Ru to the most external hydrogen-atom sphere to which a van der Waals radius of 1.20 Å has been attributed.

† The numbering of the nucleus is the same as that in the *X*-ray structures reported in Figure 2.

and ^{13}C, H_3PO_4 (85%) for ^{31}P (signals reported as positive downfield of the standard). All ^{13}C and ^{31}P n.m.r. spectra were recorded as proton-decoupled spectra. Molecular-weight determinations were made using a Wescan model 233 apparatus, based on the isopiestic method. Carbon and hydrogen elemental analyses were performed using a Perkin-Elmer 240C elemental analyser. I.r. spectra were recorded with a Perkin-Elmer 580B data system. *X*-Ray diffraction data were collected by a Philips 1100 diffractometer.

The compounds $[Ru_2(CO)_4(\mu\text{-}MeCO_2\text{-}O,O')_2(PBu^n{}_3)_2]$ (**1**),[18] $[Ru(CO)_2(MeCO_2)_2(PBu^n{}_3)_2]$ (**2**),[19] $[Ru_4(CO)_8(MeCO_2)_4(PBu^n{}_3)_2]$ (**3**),[20] $[Ru_4(\mu\text{-}H)_4(CO)_8(PBu^n{}_3)_4]$ (**4**),[6] $[Ru_4(\mu\text{-}H)_4(CO)_9(PBu^n{}_3)_3]$ (**5**),[6] and $[RuH_2(CO)_2(PBu^n{}_3)_2]$ (**6**)[3] were synthesized as reported in the literature.

Test Procedure.—All tests were performed in a stainless-steel autoclave (125 cm^3) equipped with two stopcocks and a high-pressure gauge. Air was evacuated from the vessel and then the solution of reactants was introduced by suction and the gas (nitrogen or hydrogen) from a pressure vessel up to the pressure required. Working conditions for each test are reported in Table 1 together with the results.

The reaction vessel was connected by a stainless-steel low volume (2 cm^3) coil to the i.r. cell, equipped with NaCl windows, capable of withstanding high pressure (200 atm), which could be heated to 200 °C. The coil too could be kept at the same temperature of the system. The solution present in the autoclave could therefore be transferred to the i.r. cell under reaction conditions and examined by i.r. spectroscopy. The solvent (n-heptane) bands were compensated using a variable-path i.r. cell.

Behaviour of $[Ru_2(CO)_4(\mu\text{-}MeCO_2\text{-}O,O')_2(PBu^n{}_3)_2$ *under Hydrogen*.—The experimental conditions are reported in Table 1. G.l.c. analyses, performed on the crude product using a OV1 column (35 °C for 10 min, then heated to 200 °C at 10 °C min^{-1} and then kept at 200 °C for 20 min), showed, besides the solvent peak, another one with the same retention time as that of ethyl acetate. The identity of this product as ethyl acetate was confirmed by g.l.c.–m.s. by the presence of peaks at m/z 88 $[M]^+$, 73 $[M - CH_3]^+$, 45 $[OC_2H_5]^+$, 43 $[M - OC_2H_5]^+$, 29 $[C_2H_5]^+$, 27 $[C_2H_3]^+$, and 15 $[CH_3]^+$.

Butane was detected in the crude product from another test performed in decalin and identified by g.l.c.–m.s. through peaks at m/z 58 $[M]^+$, 43 $[M - CH_3]^+$, 42 $[C_3H_6]^+$, 41 $[C_3H_5]^+$, 39 $[C_3H_3]^+$, 29 $[C_2H_5]^+$, 28 $[C_2H_4]^+$, and 27 $[C_2H_3]^+$.

Several ruthenium complexes may be recovered from these crude products as outlined below.

A solution of $[Ru_2(CO)_4(\mu\text{-}MeCO_2\text{-}O,O')_2(PBu^n{}_3)_2]$ (1.6 g, 1.91 mmol) in n-heptane (40 cm^3) was introduced into the autoclave and then hydrogen up to 170 atm at 20 °C. The vessel was heated and kept at 160 °C for 48 h. The i.r. spectrum of this solution, at room temperature under hydrogen pressure, showed, besides bands due to (**1**), a new band at 1 720 cm^{-1} which may be ascribed to the presence of free acetic acid. After 72 h at 180 °C, under the same pressure of hydrogen, the solution was cooled and the gas pressure released. New bands in the 2 200—1 500 cm^{-1} region were present.

After evaporation of the solvent under reduced pressure the solid recovered was separated by preparative t.l.c. on alumina using n-hexane as eluant. Eleven different fractions were obtained. The more consistent of them were further purified by t.l.c. or column chromatography. The following different products were recovered in the order of increasing elution times.

Compound (**11**). The product (60 mg) was collected and further purified by t.l.c. on silica gel using n-pentane as eluant. A light yellow spot was visible on the chromatographic plate using u.v. light (254 nm). Its i.r. spectrum in n-pentane showed absorptions in the 2 200—1 500 cm^{-1} range at 2 072w, 2 030vs, 2 000s, and 1 986m cm^{-1}.

N.m.r. spectra in $CDCl_3$: ^1H, τ 7.9—8.9 (m, $CH_2CH_2CH_2P$), 9.1 (t, CH_3CH_2), and 29.4 (dd, HRu, J_{HP} = 13.5, $J_{HP'}$ = 15.5 Hz); ^{31}P, 10.6 (s) and 14.0 p.p.m. (s).

$[Ru_3(\mu\text{-}H)_2(CO)_7(\mu_3\text{-}PBu^n)(PBu^n{}_3)_2]$ (**7**). A semisolid product (160 mg) was purified by t.l.c. on alumina using n-pentane as eluant. The solid gave, by crystallization from n-hexane at −80 °C, deep yellow crystals (Found: C, 42.35; H, 6.60%, *M* 1 076. Calc. for $C_{35}H_{65}O_7P_3Ru_3$: C, 42.30; H, 6.60%; *M* 994). Its i.r. spectrum in n-heptane solution, in the 2 200—1 500 cm^{-1} region, showed absorptions at 2 048s, 2 020vs, 1 988vs, 1 980s, 1 965m, 1 958(sh), and 1 939w cm^{-1}. ^1H N.m.r. in $CDCl_3$ solution: τ 7.7—8.9 (m, 42 H, $CH_2CH_2CH_2P$), 9.1 (m, 21 H, CH_3CH_2), 29.1 (dd, 1 H, HRu, $J_{HP} = J_{HP'}$ = 13.5), and 29.3 (ddd, 1 H, HRu, $J_{HP} = J_{HP'}$ = 9.0, $J_{HP''}$ = 18.0 Hz). The number of hydridic hydrogens present was evaluated by ^1H n.m.r. spectroscopy using an equimolar solution of compounds (**7**) and (**4**). The integrals of the hydridic absorptions of the two compounds gave a ratio (**7**)/(**4**) = 1/2. ^{31}P N.m.r. in $CDCl_3$ solution: δ 10.7 (d, 1 P, $PBu^n{}_3$, *J* = 97), 24.7 (s, 1 P, $PBu^n{}_3$), and 287.7 p.p.m. (d, 1 P, PBu^n, *J* = 97 Hz).

$[Ru_6(\mu\text{-}H)_6(CO)_{10}(\mu\text{-}PHBu^n)(\mu\text{-}PBu^n{}_2)_2(PBu^n{}_3)_2(\mu_6\text{-}P)]$ (**10**). The solid (80 mg) was first purified by t.l.c. on silica using n-pentane as eluant. The orange residue, after evaporation of the solvent, was dissolved in diethyl ether, methanol was then added up to incipient clouding. Upon slow evaporation of the solvent at room temperature orange-red crystals were obtained (Found: C, 39.00; H, 6.55%; *M* 1 506. Calc. for $C_{54}H_{106}O_{10}P_6Ru_6$: C, 38.00; H, 6.25%; *M* 1 708). Its i.r. spectrum in n-heptane solution, in the 2 200—1 500 cm^{-1} range, showed absorptions at 2 040vs, 2 015vs, 2 010(sh), 1 995vw, 1 972s, 1 960s, 1 950s, 1 928s, 1 922s, and 1 885vw cm^{-1}. N.m.r. spectra: ^1H ($CDCl_3$), τ 6.5 (d, 1 H, PH, J_{PH} = 330 Hz), 8.0—8.9 (m, 66 H, $CH_2CH_2CH_2P$), 9.1 (m, 33 H, CH_3CH_2), 26.2 (m, 2 H, HRu), 29.0 (m, 2 H, HRu), and 29.8 (m, 2 H, HRu); ^{31}P (CD_2Cl_2), an A_2MXB_2 spin system with signals at δ 13.7 (dd, 2 P, $PBu^n{}_3$, J_{AM} = 145), 88.7 (tdt, 1 P, P, J_{AM} = 145, J_{MX} = 13, J_{MB} = 6), 155.2 (dd, 1 P, $PHBu^n$, J_{MX} = 13, J_{XB} = 13), and 202.2 p.p.m. (dd, 2 P, $PBu^n{}_2$, J_{BX} = 13, J_{MB} = 6 Hz). These data agree with those reported previously.[3]

$[Ru_7(\mu\text{-}H)_8(CO)_{12}(\mu_3\text{-}PBu^n)(\mu\text{-}PBu^n{}_2)(PBu^n{}_3)_3(\mu_6\text{-}P)]$ (**9**). The semisolid material (220 mg) was purified by column chromatography on silica using light petroleum (b.p. 40—70 °C) as eluant. Deep brown crystals were obtained from n-pentane at −20 °C (Found: C, 37.65; H, 6.0%; *M* 1 750. Calc. for $C_{60}H_{116}O_{12}P_6Ru_7$: C, 37.50; H, 6.10%; *M* 1 922.9). The i.r. spectrum in n-heptane solution, in the 2 200—1 500 cm^{-1} range, showed absorptions at 2 048s, 2 028vs, 2 015vs, 1 983m, 1 976m, 1 966s, 1 932w, and 1 918w cm^{-1}. ^1H N.m.r. ($CDCl_3$): τ 7.9—8.9 (m, 72 H, $CH_2CH_2CH_2P$), 9.1 (m, 36 H, CH_2CH_3), 23.9 (m, 2 H, HRu), 25.1 (m, 2 H, HRu), 30.6 (m, 1 H, HRu), 31.3 (m, 1 H, HRu), 32.7 (m, 1 H, HRu), and 33.6 (m, 1 H, HRu). The number of hydridic hydrogens present was evaluated by ^1H n.m.r. spectroscopy using an equimolecular solution of compound (**9**) and (**4**). The integrals of the hydridic absorptions gave a ratio (**9**)/(**4**) = 2/1. ^{31}P N.m.r. ($CDCl_3$): δ 3.1 (d), 16.4—24.4 (m), 189.8 (s), 191.2 (s), 219.9 (t), 229.9 (t), 348.2 (s), and 353.5 p.p.m. (d). The data reported are in agreement with the formulation given.

$[Ru_2(CO)_4(\mu\text{-}MeCO_2\text{-}O,O')_2(PBu^n{}_3)_2]$ (**1**). The starting material (120 mg) was recovered.

$[Ru_6(\mu\text{-}H)_6(\mu\text{-}CO)(CO)_{12}(\mu\text{-}PBu^n{}_2)(PBu^n{}_3)_2(\mu_6\text{-}P)]$ (**8**). The semisolid material (100 mg) was purified by t.l.c. on silica using CH_2Cl_2–n-pentane (20:80) as eluant. A violet solid was recovered which was dissolved in n-pentane and crystallized at −20 °C (Found: C, 36.15; H, 5.10%; *M* 1 432. Calc. for $C_{45}H_{78}O_{13}P_4Ru_6$: C, 34.70; H, 5.05%; *M* 1 557.4). Its i.r. spectrum, in n-heptane solution, showed in the 2 200—1 500

Table 4. Experimental data for the crystallographic analyses

Compound	(7)	(8)	(9)
Formula	$C_{35}H_{65}O_7P_3Ru_3$	$C_{45}H_{78}O_{13}P_4Ru_6$	$C_{60}H_{116}O_{12}P_6Ru_7$
M	994.0	1 557.4	1 922.9
Space group	$P\bar{1}$	$P\bar{1}$	$P2_1/n$
a/Å	23.870(17)	17.785(8)	22.657(12)
b/Å	11.623(7)	21.851(9)	17.186(8)
c/Å	8.570(5)	17.087(7)	21.660(12)
α/°	87.75(1)	96.35(1)	—
β/°	86.46(1)	94.25(7)	97.43(1)
γ/°	77.79(2)	99.43(1)	—
U/Å^3	2 319(2)	6 482(5)	8 363(8)
Z	2	4	4
D_c/Mg m^{-3}	1.424	1.596	1.527
Reflections for lattice parameters, number	28	24	27
Reflections for lattice parameters, θ range/°	19.4—23.9	15.8—23.5	18.0—23.4
$F(000)$	1 016	3 104	3 880
Crystal size/mm	0.35 × 0.48 × 0.58	0.59 × 0.40 × 0.61	0.30 × 0.47 × 0.43
μ/mm^{-1}	1.086	1.483	1.367
Absorption correction (minimum, maximum)	—	0.6422, 1.4732	—
Extinction correction (minimum, maximum)	—	0.8471, 1.0100	—
Scan speed/° s^{-1}	0.10	0.10	0.075
Scan width/°	2.0	1.10	1.40
Scan mode	ω—2θ	ω—2θ	ω—2θ
θ range/°	3—24	3—25	3—24
h range	−26 to 26	−21 to 20	−25 to 25
k range	−13 to 13	−24 to 24	0—19
l range	0—9	0—19	0—24
Standard reflection	$\bar{7}\,\bar{3}\,3$	$\bar{5}\,\bar{3}\,7$	$\overline{12}\,\bar{2}\,2$
No. of measured reflections	7 226	20 375	14 011
Condition for observed reflections	$I \geqslant 3\sigma(I)$	$I \geqslant 3\sigma(I)$	$I \geqslant 2.5\sigma(I)$
No. of reflections used in refinement	4 930	10 844	6 478
Max. least-squares shift to error ratio	0.31	0.13	0.20
Min. and max. height in final difference map/e Å^{-3}	−0.16, 0.32	−0.52, 0.39	−0.21, 0.31
No. of refined parameters	484	1 448	930
$R = \Sigma\lvert\Delta F\rvert/\Sigma\lvert F_o\rvert$	0.0362	0.0526	0.0589
$R' = [\Sigma w(\Delta F)^2/\Sigma wF_o^2]^{\frac{1}{2}}$	0.0497	0.0659	0.0587
$S = [\Sigma w(\Delta F)^2/(N - P)]^{\frac{1}{2}}$*	0.9107	1.6522	1.6977
k, g in ($w = k/[\sigma^2(F_o) + gF_o^2]$)	0.9382, 0.001 13	1.7826, 0.000 986	1.7304, 0.000 127

* P = Number of parameters, N = number of observations.

cm^{-1} region, absorptions at 2 062w, 2 040vs, 2 024vs, 2 018(sh), 2 015(sh), 1 988s, 1 975m, 1 965w, and 1 765m cm^{-1}. ^{1}H N.m.r. ($CDCl_3$): τ 7.9—8.8 (m, 42 H, $CH_2CH_2CH_2P$), 9.1 (t, 21 H, CH_3CH_2), 25.1 (m, 2 H, HRu), 25.7 (dt, 2 H, HRu), and 33.6 (dd, 2 H, HRu). The number of hydridic hydrogens present was evaluated by ^{1}H n.m.r. spectroscopy using an equimolar solution of compounds (**8**) and (**4**). The integrals of the hydridic absorptions gave a ratio (**8**)/(**4**) = 3/2. ^{31}P N.m.r. ($CDCl_3$): δ 20.0 (d, 2 P, PBu^n_3, $J_{PP'}$ = 134), 197.3 (s, 1 P, PBu^n_2), and 204.3 p.p.m. (t, 1 P, P, $J_{P'P}$ = 134 Hz). The above data are in agreement with the given formulation.

$[Ru(CO)_2(MeCO_2)_2(PBu^n_3)_2]$ (**2**). Only traces of this product were separated by t.l.c.

The compound $[Ru_4(\mu\text{-}H)_4(CO)_9(PBu^n_3)_3]$ (**5**) is not detected among the products of this test. It was recovered from tests 1 and 2 of Table 1.

Crystal Structure Analysis of Compounds (**7**)—(**9**).—Table 4 summarizes the relevant data for the crystal structure analyses. The lattice parameters were refined by a least-squares procedure[21] using the Nelson and Riley[22] extrapolation function. The intensities were measured at room temperature (294 K), on a Philips 1100 diffractometer using Mo-$K_{\bar{\alpha}}$ radiation (λ = 0.710 69 Å). In no case were the intensity variations of the standard reflections >0.2%. Correction for Lorentz and polarization effects was applied and absorption was taken into account according to the azimuthal-scan method.[23]

The structure was solved by the direct methods of SHELX 76[24] for compound (**7**) and MULTAN[25] for compounds (**8**) and (**9**). Refinement was by block-diagonal least squares on F, using SHELX 76.

As frequently happens with hydrocarbon linear chains, disorder was found for the terminal methyls of some of the butyl chains. In spite of this disorder and of the presence of the heavy ruthenium atoms, many hydrogen atoms were localized in the final electron-density difference maps. These atoms were refined isotropically, but, at the end of the analysis for the geometrical calculations needed for the discussion of the structures, all the hydrogen atoms were considered in the calculated positions.

In the crystals of compound (**8**) the two crystallographically independent molecules are, in the unit cell, related by a pseudo-two-fold screw axis running along the [4 1 0] direction at z = 0.30 and with a translation of about $\frac{1}{2}a$. The correctness of the space-group choice was checked using the TRACER[26] program, the NIGGLI and SYMMOL routines of the PARST[27] program, and the MISSYM[28] routine of the NRCVAX[29] system of programs.

The atomic scattering factors and the anomalous-scattering coefficients were from ref. 30. The calculations were carried out on the GOULD-SEL 32/77 computer of the 'Centro di Studio per la Strutturistica Diffratometrica del C.N.R. (Parma)' and on the CRAY XMP1 computer of the 'Centro Interuniversitario di Calcolo dell' Italia Nord Orientale (CINECA, Casalecchio, Bologna). In addition to the quoted programs, THMV,[31] ORTEP,[32] and PLUTO[33] were used.

Throughout this paper the averaged values are means weighted according to the reciprocals of the variances and the corresponding estimated standard deviations (e.s.d.s) are the largest of the values of the 'external' and 'internal' standard deviations.[34]

Additional material available from the Cambridge Crystallographic Data Centre comprises H-atom co-ordinates, thermal parameters, and remaining bond lengths and angles.

Acknowledgements

We thank Consiglio Nazionale delle Ricerche and Ministero della Pubblica Instruzione for financial support. The authors are indebted to Professor C. Guastini for collection of intensity data, to Dr. M. Lanfranchi for his help with graphical problems, and to Professor A. Scrivanti (University of Venice) for helpful discussion of some n.m.r. spectra.

References

1 M. Bianchi, G. Menchi, F. Francalanci, F. Piacenti, U. Matteoli, P. Frediani, and C. Botteghi, *J. Organomet. Chem.*, 1980, **188**, 109.
2 U. Matteoli, M. Bianchi, G. Menchi, P. Frediani, and F. Piacenti, *J. Mol. Catal.*, 1984, **22**, 353.
3 P. Frediani, M. Bianchi, A. Salvini, F. Piacenti, S. Ianelli, and M. Nardelli, *J. Chem. Soc., Dalton Trans.*, 1990, 165.
4 P. Frediani, U. Matteoli, G. Menchi, M. Bianchi, and F. Piacenti, *Gazz. Chim. Ital.*, 1985, **115**, 365.
5 P. Frediani, M. Bianchi, F. Piacenti, S. Ianelli, and M. Nardelli, *Inorg. Chem.*, 1987, **26**, 1592.
6 F. Piacenti, M. Bianchi, P. Frediani, and E. Benedetti, *Inorg. Chem.*, 1971, **10**, 2759.
7 W. C. Hamilton, *Acta Crystallogr.*, 1965, **18**, 502.
8 A. G. Orpen, *J. Chem. Soc., Dalton Trans.*, 1980, 2509.
9 V. Schomaker and K. N. Trueblood, *Acta Crystallogr., Sect. B*, 1968, **24**, 63.
10 S. B. Colbran, B. F. G. Johnson, J. Lewis, and R. M. Sorrell, *J. Chem. Soc., Chem. Commun.*, 1986, 525.
11 C. Bergounhou, J-J. Bonnet, P. Fompeyrine, G. Lavigne, N. Lugan, and F. Mansilla, *Organometallics*, 1986, **5**, 60.
12 P. E. Garrou, *Chem. Rev.*, 1985, **85**, 171.
13 C. A. Tolman, *Chem. Rev.*, 1977, **77**, 313.
14 J. L. Petersen and R. P. Stewart, jun., *Inorg. Chem.*, 1980, **19**, 186.
15 S. Sabo, B. Chaudret, and D. Gervais, *J. Organomet. Chem.*, 1983, **258**, C19.
16 H. C. Foley, W. C. Finck, C. J. Pierpont, and G. L. Geoffroy, *Organometallics*, 1982, **1**, 1379.
17 D. W. Krassowski, J. H. Nelson, K. R. Brower, D. Hauenstein, and R. A. Jacobson, *Inorg. Chem.*, 1988, **27**, 4294 and refs. therein.
18 G. R. Crooks, B. F. G. Johnson, J. Lewis, I. G. Williams, and G. Gamlen, *J. Chem. Soc. A*, 1969, 2761.
19 M. Bianchi, P. Frediani, U. Matteoli, G. Menchi, F. Piacenti, and G. Petrucci, *J. Organomet. Chem.*, 1983, **259**, 207.
20 M. Bianchi, U. Matteoli, P. Frediani, F. Piacenti, M. Nardelli, and G. Pelizzi, *Chim. Ind.* (*Milan*), 1981, **63**, 475.
21 M. Nardelli and A. Mangia, *Ann. Chim.* (*Rome*), 1984, **74**, 163.
22 J. B. Nelson and D. P. Riley, *Proc. Phys. Soc. London*, 1945, **57**, 160, 477.
23 A. C. T. North, D. C. Phillips, and F. Scott Mathews, *Acta Crystallogr., Sect. A*, 1968, **24**, 351.
24 G. M. Sheldrick, SHELX 76, Program for Crystal Structure Determination, University of Cambridge, 1976.
25 P. Main, S. J. Fiske, S. E. Hull, L. Lessinger, G. Germain, G. P. Declercq, and M. M. Woolfson, MULTAN 80, A System of Computer Programs for the Automatic Solution of Crystal Structures from *X*-Ray Diffraction Data, Universities of York and Louvain, 1980.
26 S. L. Lawton and R. A. Jacobson, 'The Reduced Cell and its Crystallographic Applications,' United States Atomic Energy Commission, Research and Development Report, Chemistry (UC-4), TID-4500, Ames Laboratory at Iowa State University of Science and Technology, 1965.
27 M. Nardelli, *Comput. Chem.*, 1983, **7**, 95.
28 Y. Le Page, *J. Appl. Crystallogr.*, 1987, **20**, 264.
29 E. J. Gabe, F. L. Lee, and Y. Le Page, in 'Crystallographic Computing 3: Data Collection, Structure Determination, Proteins and Databases,' eds. G. M. Sheldrick, C. Krüger, and R. Goddard, Clarendon Press, Oxford, 1985, p. 167.
30 'International Tables for *X*-Ray Crystallography,' Kynoch Press, Birmingham, 1974, vol. 4, pp. 99 and 149.
31 K. N. Trueblood, THMV, University of California, Los Angeles, 1984.
32 C. K. Johnson, ORTEP, Report ORNL-3794, Oak Ridge National Laboratory, Tennessee, 1965.
33 W. D. S. Motherwell and W. Clegg, PLUTO, University of Cambridge, 1976.
34 H. Topping, 'Errors of Observation and Their Treatment,' Chapman & Hall, London, 1960, pp. 87 and 91.

Received 2nd June 1989; *Paper* 9/02307K